

LRP 626/98

December 1998

DIBORANE NITROGEN/AMMONIA PLASMA
CHEMISTRY INVESTIGATED BY INFRARED
ABSORPTION SPECTROSCOPY

D. Franz, M. Hollenstein, Ch. Hollenstein

submitted for publication to
J. of Physical Chemistry B

Diborane nitrogen/ammonia plasma chemistry investigated by infrared absorption spectroscopy

D. Franz^{*}, M. Hollenstein and Ch. Hollenstein

Centre de Recherches en Physique des Plasmas,
Ecole Polytechnique Fédérale de Lausanne,
PPB Ecublens, CH-1015 Lausanne, Switzerland

Abstract.

Boron nitride films were deposited by rf capacitively-coupled plasma (13.56 MHz) using two different gas mixtures: Ar-B₂H₆-NH₃ and Ar-B₂H₆-N₂. In order to study the gas-phase reactions of the plasma *in situ* Fourier transform infrared absorption spectroscopy (FTIR) has been used. The study reveals that, in our conditions, mixing ammonia with diborane leads to the well known creation of diammoniate of diborane. In the presence of the plasma, salt production is inhibited and creation of aminoborane is observed. Replacing ammonia by nitrogen, none of these species could be detected. The mechanism of formation of these products from the precursors and their influence on the deposited film are also discussed.

* e-mail: david.franz@epfl.ch, phone number: ++41 21 693 34 97, fax number ++41 21 693 51 76

1. Introduction.

In recent years, both physical (PVD) and chemical (CVD) vapour deposition techniques have been used for the synthesis of boron nitride (BN) thin films^{1,2}. Boron nitride is chemically and thermally stable and insulating. Boron nitride has several crystalline structures similar to the structures in carbon. Cubic boron nitride (c-BN) has many outstanding properties such as wide band-gap, chemical inertness, high thermal conductivity and hardness comparable to diamond. Hexagonal BN (h-BN) has a layered structure similar to graphite, but is a transparent, very refractory corrosion-resistant material with good dielectric properties. In addition amorphous, turbostratic and wurtzite phases can be found^{1,2}.

Because of these properties, the deposition of boron nitride thin films has been widely investigated, motivated by their potential for hard coatings for wear resistance, for optical coatings and for high temperature electronic devices. Up to now only few CVD deposition processes³⁻⁶ have been developed due to the complexity of obtaining c-BN coatings with these techniques. Literature gives some recipes with many different boron precursors such as diborane⁶, borane ammonia complexes⁷, borazine⁸ or boron trichloride⁹ but little investigation of the plasma chemistry were done. An understanding of the basic chemistry in the plasma is crucial to achieve a CVD deposition technique for industrial applications. This article deals with a study of the chemical processes in a deposition plasma of boron nitride films with diborane gas as boron precursor and ammonia or nitrogen gases as nitrogen precursors.

Plasma-enhanced chemical vapour deposition (PECVD) is a technique for the deposition of a wide variety of films by breaking down gaseous precursors into radicals which deposit onto the substrate. Owing to the complexity of the PECVD processes, the properties of

the films depend strongly on the particular deposition scheme and the gas chemistry used. The first step in the control of plasma deposition is the understanding of the mechanisms in the gas phase. *In situ* Fourier transform infrared absorption spectroscopy (FTIR) of the gas phase is a useful non-perturbative diagnostic to reach a better understanding of the plasma chemistry. In particular, gas composition ¹⁰, formation of new species (gas or particle ¹¹), reactive gas consumption ¹² and gas temperatures ¹³ can be measured by this technique.

In this paper, BN films have been deposited by rf capacitively-coupled plasma with gas mixtures of Ar-B₂H₆-NH₃ and Ar-B₂H₆-N₂ under various preparation conditions. The gas-phase reactions in the plasma and the deposited BN films were both investigated by FTIR absorption spectroscopy as function of the gas composition.

2. Experimental arrangement.

The experiments were performed in a rf capacitively-coupled plasma at 13.56 MHz with 130 mm diameter electrodes (figure 1). The distance between the stainless steel electrodes is 30 mm. To avoid reaction of diborane with ammonia in the gas line, these gases were carried to the reactor by two separate gas lines. The experiments were carried out with a rf power of 75 W and a pressure of 0.5 mTorr. The reactor walls were heated to 80 °C and the grounded electrode was heated to 200 or 400°C. To better confine the plasma between the electrode space, a shield was placed around these electrodes. The BN coatings were deposited on a single-polished face Silicon (100) wafer placed on the grounded electrode. As a safety precaution, the resultant gases at the exhaust were passed through a commercial gas scrubber. For the BN deposition films, the plasma was switched on after the injection of all the gases (diborane, argon and ammonia or nitrogen) and after the regulation of the working pressure. The pressure is automatically controlled by feedback to the speed of the turbomolecular pump.

For the *in situ* infrared absorption measurements, ZnSe windows were mounted on diametrically opposite flanges. The spectra were measured using a Bruker IFS-55 spectrometer with a glow bar source and an external detector. The parallel beam leaving the spectrometer is directed through the plasma (single pass) and is focused by an off-axis parabolic gold mirror onto a liquid nitrogen cooled mercury-cadmium-telluride (MCT) detector (Graseby type FTIR W24). The Fourier transform of the detector signal yields the spectrum in the 500-4000 cm^{-1} range with a chosen spectral resolution of 1 cm^{-1} . To obtain reasonable signal to noise ratio, the measurements were performed by averaging over one thousand spectra. To minimize the influence of water and CO_2 absorption bands in the spectra, the infrared light path, including the detection systems, were enclosed and continuously flushed with pure nitrogen gas. Spectra were acquired before and after each measurement to check for variations in the source intensity and/or the detector sensitivity. The reference spectra used were acquired after the measurements in order to correct the influence of possible deposition on the ZnSe windows.

The structure of BN films was investigated using *ex-situ* FTIR absorption spectroscopy. The composition of the deposited films was measured using XPS.

3. Results.

Diborane and ammonia: IR absorption bands.

In order to investigate the influence of the gas mixture on the gas phase reactions and coating properties, the diborane/argon (15% diborane in argon) flow was altered while keeping the ammonia (or nitrogen) flow constant. Constant total flow was maintained by adjusting the argon flow. To investigate the effect of nitrogen precursor, ammonia was also replaced by nitrogen. The deposition conditions are summarized in Table I.

The use of group theory for the diborane (D_{2h}) and the ammonia (C_{3v}) molecules yields the two following irreducible representations:

$$\Gamma_{\text{vib}}(\text{B}_2\text{H}_6) = 4A_g + 2B_{1g} + B_{2g} + 2B_{3g} + A_u + 2B_{1u} + 3B_{2u} + 3B_{3u}$$

$$\Gamma_{\text{vib}}(\text{NH}_3) = 2A_1 + 2E$$

We therefore expect a maximum of 8 IR bands (only B_{1u} , B_{2u} and B_{3u} are IR active) for pure diborane and 6 for pure ammonia. Nitrogen gas, being a diatomic homonuclear molecule, is infrared inactive.

Indeed Figures 2 a) and b) show the infrared transmitted signal, in a spectral range of 500-3600 cm^{-1} through diborane/argon and pure ammonia gas before mixing. The diborane bridge absorbs very strongly at 1660-1500 cm^{-1} due to asymmetric in-phase hydrogen motion. The other strong absorption bands are due to the BH or BH_2 groups. For ammonia, the stronger bands absorption are due to the NH groups. A list of the absorption regions and their mode assignments can be found in table II ¹⁴.

The band absorption due to the diborane bridge can be used to estimate the degree of dissociation of the diborane in the plasma. If this absorption band overlaps with another one of the reactant (such as ammonia) or any new species created in the gas phase, it is no longer possible anymore to have any estimation. The integrated surface

($S_{absorption} = \int_{1500\text{ cm}^{-1}}^{1660\text{ cm}^{-1}} (1 - T(\sigma)) d\sigma$) of the band is proportional to $(1 - \exp(-\beta n))$, where n is the number density of the absorbing gas and $\beta = k(\nu)l$, where l is the optical path and $k(\nu)$ is the absorption coefficient. This relation is not exact because the 1 cm^{-1} resolution is not sufficient to completely resolve the individual gas lines. As shown by Cleland *et al*¹⁵, this lack of resolution results in a non-linear relation between the measured transmittance and the true transmittance of the lines and consequently, the Beer and Bouguer law can be used only to have a rough estimation of the degree of dissociation of the gas. The consumption (depletion) of diborane due to its dissociation in the plasma phase is obtained by dividing the integrated band in presence of plasma and the integrated band of the gas mixture and by developing the exponential to first order:

$$\frac{S_{absorption}(\text{plasma})}{S_{absorption}(\text{gas})} = \frac{1 - \exp(-\beta n(\text{plasma}))}{1 - \exp(-\beta n(\text{gas}))} \cong \frac{n(\text{plasma})}{n(\text{gas})} = 1 - \text{depletion} \quad (1)$$

To have a better estimation of the gas depletion, in principle a more accurate method¹² can be used; however the necessary calibration is prohibitively difficult in our case because of the problem of combined dilution (diborane in argon) and gas-dependant pumping speed of the turbomolecular pump.

Diborane/nitrogen mixture: IR absorption in the gas phase.

The infrared transmission spectra of the diborane, argon and nitrogen mixture is shown on Fig 3a. The decrease of the intensity of the absorption bands in comparison with Fig. 2a is the consequence of the decrease of the partial pressure of diborane due to the dilution with nitrogen and argon. Since the nitrogen is infrared inactive, and no gas reaction takes place, no new absorption bands appear.

Diborane/ammonia mixture: IR absorption in the gas phase.

In contrast, the infrared transmitted signal of the mixing of diborane, argon and ammonia shows new absorption bands at different regions coming from the gas phase

reactions without plasma (see figure 4a and 5c). Adding ammonia to diborane results in the formation of different species depending on the temperature range and on the mixing ratio. At room temperature a stable white solid borohydride, the diammoniate of diborane $[\text{H}_2\text{B}(\text{NH}_3)_2]^+[\text{BH}_4]^-$, is produced (see table III ¹⁶⁻¹⁹). At temperatures higher than 200°C, the ring compound borazine is produced along with some polymeric material such as $(\text{BNH}_2)_n$. Increasing the temperature progressively removes hydrogen, thereby forming polymeric $(\text{BNH})_n$ and finally BN ¹⁷.

At room temperature another BN compound can be produced from the reaction between ammonia and diborane: the 1:1 adduct $\text{BH}_3 \cdot \text{NH}_3$ ¹⁸. However, this white solid sublimates just above room temperature. It therefore unlikely for this compound to be detected in our case because of the high temperatures used. Heating this adduct leads to the elimination of H_2 to form aminoborane ($\text{H}_2\text{B}=\text{NH}_2$) ¹⁹.

In order to investigate the temperature effect on the creation of new species, experiments were performed at 400°C and 200°C with the same gas mixture (28 sccm of diborane/argon mixture (15% diborane in Argon) and 36 sccm of ammonia). The two spectra obtained at 200°C and at 400°C are shown in figure 4. The spectra still show the absorption bands of the reactants (diborane and ammonia) and some new bands. Due to the overlapping of the gas absorption bands in the region of the diborane bridge, no value of the depletion of diborane can be deduced as in the case of the diborane/nitrogen mixture. At 200°C, a strong decrease of the transmitted signal with the wavenumber is observed. This decrease is due to elastic Mie scattering of the beam by solid particles in the gas phase. At 400°C, the density and/or size of the solid particles is too low to observe this phenomena. The new broad absorption bands are the fingerprint for the creation of solid particles of diammoniate of diborane $[\text{H}_2\text{B}(\text{NH}_3)_2]^+[\text{BH}_4]^-$ ²⁰. The absorption bands between 3100 and 3250 cm^{-1} are attributed to the NH (antisymmetric and symmetric) stretch of NH_3 . Two BH stretching modes

of the BH_4^- anion²¹ were observed between 2300 cm^{-1} and 2400 cm^{-1} . In the region between 1400 and 1660 cm^{-1} we observe an overlapping between the absorption bands of the reactants and probably new NH_3 (symmetric and antisymmetric) bending modes²². The very strong absorption at 1370 cm^{-1} is due to the NH_3 symmetric bending. The bands between 1000 and 1200 cm^{-1} are attributed to the bending mode of the BH_4^- anion or may be assigned to the H-B-H bending mode of the cation²⁰. Finally, a new band with respect to the spectrum of pure ammonia is present at 780 cm^{-1} which most probably can be assigned to NH deformation. The observed absorption bands are summarized in table IV^{18,20-22}. The spectrum recorded at 400°C shows some of the bands encountered in the spectrum described previously but their intensities are weaker. This decrease is partly due to the decrease of the reactant density due to the increase of temperature at constant pressure but also due to the fact that aminoborane ($\text{H}_2\text{B}=\text{NH}_2$) has been synthesised. The only bands which do not overlap with the absorption bands of the reactants and with the diammoniate of diborane are weak bands at 1338 cm^{-1} (B=N stretch)²⁰ and 608 cm^{-1} (BH_2 rock)²⁰ (see figure 6c) suggesting that some of this product has been created. There is no evidence for creation of other BN compounds such as borazine. Table V summarizes the absorption band of aminoborane¹⁸⁻²².

Figure 6 shows the influence of the gas mixture ratio. In our case, the ratio between the diborane and the ammonia flux remains always lower than a quarter in order to deposit films with a B:N ratio lower than 3. In this range, all spectra show the same absorption bands but at different intensities linked with the density of diborane influencing the density of species created.

Diborane/nitrogen mixture: IR absorption in the plasma phase.

In the spectra in presence of plasma in a diborane, argon and nitrogen mixture (figure 3b), we observe a strong decrease of all the absorption bands (BH_x ($x=1,2$) and $\text{B}\cdot\cdot\text{H}\cdot\cdot\text{B}$). This is a consequence of diborane dissociation. Using (1) we can approximately estimate the

depletion of diborane at about 70 %. Due to the high surface reactivity of the radicals created (BH_y , $y \leq 4$), their density in the plasma remains relatively low and consequently gives rise to low absorption band intensities. Moreover, due to the dissociation mechanism, their rotational and vibrational temperatures may be high which gives less absorption because of the reduced ground state population²³. In the whole spectral range, no indication of B-N absorption band could be detected.

Diborane/ammonia mixture: IR absorption in the plasma phase.

Strong modifications must be indicated in the case of diborane, argon and ammonia mixing in presence of plasma (figure 4b and 5d). Most of the modifications of the spectra can be understood in term of disappearance of the salt creation in the gas phase and creation of new B-N species such as double bonded B=N species (aminoborane) and the dissociation of the reactants (diborane and ammonia). In Fig. 4b, 5d and 6b, the spectra are similar and no presence of the $[H_2B(NH_3)_2]^+[BH_4]^-$ is observed even at 200°C. It must be pointed that in presence of plasma, surface temperature seems not to play any significant role, opposite to the case with only the gas mixture. There is no more evidence of diborane in the absorption spectra due to the overlapping with new absorption bands coming from aminoborane. The spectra reveal a weak but non negligible absorption in the range between 3400-3520 cm^{-1} which might be attributed to NH stretch in aminoborane^{19,20}. The dissociation of diborane and ammonia and the creation of aminoborane in the plasma also lead to strong modification of the absorption bands in the region between 2740 and 2450 cm^{-1} , due to the BH symmetric and antisymmetric stretching modes and in the region between 1500 and 1680 cm^{-1} , due to the NH_2 symmetric bending mode of aminoborane. Absorption bands at 608 cm^{-1} (BH_2 rock) and at 1338 cm^{-1} (B=N stretching) (see figure 5d) confirm the increase of the density of aminoborane. This last band is the most significant absorption band of the aminoborane because it does not overlap with any other absorption bands of the reactants. The origin of the

absorption band at 1450 cm^{-1} is not clear. It may be not attributed to aminoborane^{19,20}. The general range of absorption of the covalent B-N bond compounds is in the $1550\text{-}1330\text{ cm}^{-1}$ region so that the broad band absorption at 1450 cm^{-1} could be probably due to a B-N vibration. Borazine has a strong absorption band (B=N stretching) in that region²⁴ but there is no other evidence of presence of this compound because of its strong overlapping with the aminoborane and reactants bands.

In the diborane/ammonia mixture in presence of plasma, keeping the walls and electrode temperature constant leads to the creation of species which are normally not observed at these temperatures. This is due to the extra energy brought to the gas by the plasma and the creation of highly reactive radicals ($BH_y, NH_z, y \leq 4, z \leq 2$) induced by electron collisions in the plasma. In the case of diborane and nitrogen mixing, the dissociation rate of the triple bonded nitrogen molecule by direct electron impact is very low due to the high energy needed for that process²⁵ (24.3 eV). In our parameter range, the mean electron energy (T_e) is a few eV. Assuming a Boltzmann distribution of the electron energy distribution function, only a few electrons (about 10 per million with $T_e = 2\text{ eV}$) will have sufficient energy to dissociate nitrogen. Moreover, molecular nitrogen does not react spontaneously with diborane, so that only few chemical reactions take place in this kind of plasma.

Summary.

When using nitrogen and diborane gases as precursors, no gas phase reactions take place between the two gas precursors. In the presence of plasma in our conditions, no $B_xN_yH_z$ could be detected by FTIR absorption spectroscopy. Only the decrease of the diborane density due to dissociation is observed. In contrast, mixing ammonia and diborane gases as precursors leads to rich gas phase reactions. Diammoniate of diborane $[H_2B(NH_3)_2]^+[BH_4]^-$ and some aminoborane ($H_2B=NH_2$) are produced. Switching on the plasma results in the disappearance

of this salt and the density of aminoborane is increased. Using nitrogen as gas precursor, the very low plasma chemistry means that the key to understanding the growth of the film is in the plasma-surface interactions, such as bombardment and surface reactivity. When using ammonia as gas precursors, due to the B-N bondings created in the plasma, plasma chemistry must also be taken in account to understand the deposition processes.

Coatings.

All the films were grown on the grounded electrode at a temperature of 400 °C. They show a mirror-like aspect and have good adhesion. The film thickness varies from 90 to 190 nm. The thickness of the films decreases with increasing diborane flux. The nature of the deposited film was first investigated by using *ex situ* infrared spectroscopy. Fig 7 shows the FTIR spectra of the different films produced under the conditions of table I. The main features are a strong asymmetric band near 1380 cm⁻¹, related to B-N stretching vibration (in-plane) and a weaker band near 780 cm⁻¹, related to the B-N-B bending mode (out-of plane). There are the characteristic absorption bands of sp² bonds in BN films. The IR spectrum also contains other absorption bands listed in table VI confirming the presence of B-H, N-H and sp³ bonds in the film.

In our conditions, no cubic (sp³ bonds) BN films could be obtained. In fact, the ion current density and boron arrival rate play a central role for the stabilization of the hard phase¹. In our conditions, the plasma potential is limited to about 50 V ($[V_{rf}-V_{sb}]/2$, table I), but due to collisions in the sheath which can not be neglected at our pressure (0.5 Torr) the mean bombardment energy of ions on the substrate placed on the grounded electrode is much less than 50 eV. This energy is probably not high enough to promote sp³ bonding. Moreover, the plasma power was low and no external magnetic field was used to increase the plasma and the ion current density⁶.

The films deposited with the diborane/nitrogen mixture show only BH absorption bands at high diborane/ammonia ratio. On the contrary, the NH absorption band is always observed in the diborane/ammonia mixture and is probably linked to NH_x -containing species created in the plasma. In the diborane/nitrogen mixture no NH at all is observed. This is a consequence of the poor chemical reaction in the plasma and the low concentration of hydrogen, coming only from the diborane.

Figure 8 shows the influence of the diborane/argon flux on the deposition rate and the B:N ratio of the surface of the film obtained by XPS. For fluxes less than 30 sccm, there is a linear increase of the deposition rate whereas the B:N ratio remains more or less constant, equal to 1:1. In that region the diborane flux limits the deposition rate of the film. For higher flux values, the deposition rate increases whereas the B:N ratio strongly increases. In that case, the ammonia flux does not limit the film deposition rate and the lack of N-containing species causes boron rich films. Modifying the diborane flux allows the control of the deposition of graded layers. For example it is possible to start with boron rich films to obtain better adhesion of the film at the interface⁵ and then to continuously change the fluxes to achieve a B:N ratio equal to 1 to allow the growth of the cubic phase²⁶.

Keeping all the parameters constant and replacing ammonia by nitrogen leads to a strong increase of the deposition rate (a factor 20 at the lowest diborane flux) with an increase of the B:N ratio from 0.97 to 2.5 showing the requirement of a very low diborane dilution in nitrogen plasma to achieve a 1:1 B:N ratio. When using nitrogen, the incorporation of N atoms in the growing film is mainly due to surface reactions of ionized molecular nitrogen impinging on the surface, whereas with ammonia, N- and B-containing species already exist in the plasma. The decrease of the deposition rate of the BN films when replacing nitrogen by ammonia is probably due to the creation of BN (aminoborane) compounds in the plasma phase. With nitrogen, the radicals created (BH_y , $y \leq 4$) can participate directly in the

deposition, whereas with ammonia, many of these species react in the plasma to create BN compounds. Thus, a fraction of the B-containing radicals issued from the decomposition of the diborane could still directly deposit, whereas the rest participate in an intermediate step to create BN compounds which can be pumped out or can react in the plasma phase and create BN-containing radicals which can participate to the deposition.

4. Conclusions.

In situ Fourier transform infrared absorption spectroscopy (FTIR) has been used to investigate diborane, ammonia/nitrogen, argon mixtures in capacitively coupled rf plasmas. Useful information on the gas phase chemistry can be deduced from the measured infrared spectra. The creation of the well known stable white solid borohydride, the diammoniate of diborane has been observed when mixing diborane with ammonia. Increasing the reactor temperature decreases strongly its formation and allows the formation of other BN species, such as aminoborane. The presence of plasma leads to a new chemistry different from the gas phase chemistry. This is the consequence of the creation of reactive radicals produced by electron collisions in the plasma. The presence of the plasma leads to an increase of the aminoborane production while the previous salt production is removed.

All the films deposited in our conditions were sp^2 bonded and some absorption bands due to BH, NH and sp^3 bonds could be detected. Replacing nitrogen by ammonia leads to different processes in the plasma influencing the deposition. In fact, the use of ammonia leads to rich chemical reactions in the plasma that must be taken into account to explain the film growth, whereas using nitrogen, the plasma-film interactions dominate the growth due to the weak plasma chemistry. In our case, even with the creation of BN species in the plasma, no cubic BN films could be deposited. Further investigations, mixing diborane and ammonia at low dilution in a hydrogen plasma will be done in order to study the hydrogen effect on the plasma chemistry and in the stabilization of the cubic phase ³.

In our experiments the power was limited at 75 W, but it should be very useful to increase the rf power in order to increase the hydrogen elimination in the $B_xN_yH_z$ compounds created by the reaction between ammonia and diborane. In our case, at low rf power aminoborane is produced ($H_2B=NH_2$) and the power increase should allow the creation of borazine ($B_3N_3H_6$), then BNH compounds and finally non-hydrogenated BN species. Further investigations in this direction should be very helpful to understand the influence of the chemistry that take place in the plasma CVD processes and its influence on BN films properties. Moreover, the use of FTIR absorption spectroscopy with other boron precursors, such as boron trichloride (BCl_3), borazine ($B_3N_3H_6$) or borane ammonia complexes (BH_3NH_3) in conditions allowing the deposition of the hexagonal and cubic phase of BN should give much information on the importance of the plasma chemistry in the stabilization of the hard phase.

Acknowledgments.

The authors would like to thank Dr. J. Patscheider for the XPS analysis of the films, L. Chevalley for participation in the measurements and A. A. Howling for many fruitful discussions This work was supported by the Swiss Priority Program on Materials research, project 3.3D.

References.

- (1) Hackenberger, L.B; Pilipone L. J.; Messier, R., *Science and Technology of Thin films*, World scientific, Singapore, 1995; 121
- (2) Karim M. Z.; *et al.*, *Materials and Designs*, **1992**, *13*, 207
- (3) Konyashin, I.; *et al.*, *Thin Solid Films*, **1997**, *308-309*, 101
- (4) Saitoh, H.; Yarborough, W. A., *Diamond and Related Materials*, **1992**, *3*, 137
- (5) Murakawa, M.; Watanabe, S., *Surf. and Coat. Technol.*, **1990**, *43/44*, 145
- (6) Dworschak, W.; Jung, K; Erhardt, H., *Thin Solid Films*, **1995**, *254*, 65
- (7) Karim, M. Z.; *et al.*, *Surface Coatings Technol.*, **1991**, *49*, 416
- (8) Nguyen, S. V.;*et al.*, *J. Electrochem. Soc*, **1994**, *141*, 1633
- (9) Matsumoto, S.; Nishida, N.; Akashi, K; Sugai, K., *Journal of Mat. Science*, **1996**, *31*, 713
- (10) Courteille, C.; *et al.*, *41st Annual Technical Conference Proc. of the Soc. of Vacuum Coaters*, Boston, 1998, 327
- (11) Hollenstein, C.; *et al.*, *Journal of Physics D: Applied Physics*, **1988**, *31*, 74
- (12) Sansonnens, L.; Howling, A. A.; Hollenstein, Ch., *Plasma Sources Sci. Technol.*, **1998**, *7*, 114
- (13) Haverlag, M.; de Hoog, F.J.; Kroesen, G. M. V, *J. Vac. Sci. Technol.*, **1991**, *A9(2)*, 327
- (14) Socrates, G., *Infrared Characteristics Group Frequencies*, Wiley, New York, 1997
- (15) Cleland, T. A.; Hess, D. W., *J. Appl. Phys.*, **1988**, *64*, 1068
- (16) Gomez-Aleixandre,C.; *et al*, *J. Phys. Chem*, **1993**, *97*, 11043
- (17) Rand, M. J.; Roberts, J. F., *J. Electrochem. Soc*, **1968**, *115*, 423
- (18) Carpenter, D.; Ault, B. S., *Chem. Phys. Lett.*, **1992**, *197*, 171
- (19) Gerry, M. C. L.; Lewis-Bevan, W.; Merer, A. J.; Westwood, N. P. C.; *J. Mol. Spectrosc.*, **1985**, *110*, 153
- (20) Carpenter, D.; Ault, B. S.; *J. Phys. Chem.*, **1991**, *95*, 3502

- (21) Emery, A. R; Taylor, R. C.; J. Phys. Chem., **1958**, 28, 1029
- (22) Nakamoto, K., *Infrared and Raman spectra of Inorganic and Coordination Compounds* 4th ed., Wiley-Interscience, New York, 1986
- (23) Knights, J. C.; Schmitt, J.; Perrin; J.; Guelachvili, G.; J. Phys. Chem., **1982** 76, 3414
- (24) Kaldor, A.; Porter, R. F., *Inorganic Chemistry*, **1971**, 10(4), 775
- (25) von Engel, A., *Electric Plasmas : their nature & uses*, Taylor and Francis Ltd, London, 1983
- (26) Hackenberger, L.B.; Pilipone, L. J.; Messier, R.; Lamaze, G.P., J. Vac. Sci. Technol., **1994**, A12(4), 1569

Table I. Deposition conditions of the BN films with the two different mixtures.

Table II. Band positions and Assignments for pure diborane and ammonia.

Table III. Compounds created with a diborane ammonia mixture.

Table IV. Band positions and Assignments for $[\text{H}_2\text{B}(\text{NH}_3)_2]^+[\text{BH}_4]^-$.

Table V. Band positions and Assignments for aminoborane.

Table VI. Infra red absorption of the BN films.

Figure 1. Schematic top view of the infrared absorption spectroscopy (FTIR) arrangement.

Figure 2. Infrared transmitted spectra of a) diborane/argon mixture and b) pure ammonia.

Figure 3. Infrared transmitted spectra through a) the gas and b) the plasma of a diborane/argon and nitrogen mixture (56 and 40 sccm). The spectrum b) is shifted for clarity.

Figure 4. Infrared transmitted spectra for a diborane/argon, argon and ammonia gas mixture (56 and 36 sccm) through a) the gas and b) the plasma for two different grounded electrode temperatures 200 and 400 °C. The spectra are shifted for clarity.

Figure 5. Infrared transmitted spectra through a) diborane/argon mixture b) pure ammonia. Spectra c) and d) are the spectra of a diborane/argon and ammonia mixture (56 and 36 sccm at 400 °C) through the c) gas and d) the plasma. The spectra are shifted for clarity.

Figure 6. Infrared transmitted spectra through a) the gas and b) the plasma of a diborane/argon, argon and ammonia mixture gas for different diborane/argon fluxes, 1) 7, 2) 14, 3) 28, 4) 56 sccm, see Table I. The spectra are shifted for clarity.

Figure 7. Infrared spectra of boron nitride films deposited at 400°C for different diborane/argon fluxes 1) 7, 2) 14, 3) 28, 4) 56 sccm with ammonia. Spectrum 0) is obtained from the film deposit under nitrogen gas, see Table I). The spectra are shifted for clarity.

Figure 8. Evolution of the deposition rate and the B/N ratio for the BN films deposited under the conditions of table I.

Table I.

Mixture	$B_2H_6-NH_3$	$B_2H_6-N_2$
Rf power density (W/cm^2)	0.57	0.57
V_{rf}/V_{sb} [V]	250/150	230/145
Substrate temperature [$^{\circ}C$]	400	400
Gas pressure (mTorr)	0.5	0.5
B_2H_6 (15 % in Argon) (sccm)	7, 14, 28, 56	56
NH_3/N_2 (sccm)	36/0	0/40
Deposition rate ($\text{\AA}/s$)	0.18-0.65	3.8

Table II.

Wavenumber [cm^{-1}]	Band assignment
	Diborane
972	BH_2 wagging
1173	B-H in-plane def (free hydrogen)
1601	$B \cdot H \cdot B$ (bridged hydrogen) asym in-phase motion of H atom
1869	$B \cdot H \cdot B$ sym out-of-phase motion of H atom
2519	B-H str
2592	BH_2 asym stretch
2625	BH_2 sym stretch
	Ammonia
932	N-H symmetrical bend
967	N-H symmetrical bend
1626	N-H asymmetrical bend
3336	N-H in-phase stretch
3443	N-H out-of-phase stretch

Table III.

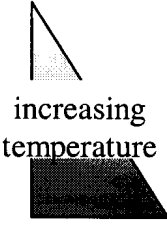
Room Temperature	$B_2H_6 + NH_3 \rightarrow H_3B \cdot NH_3$
	$B_2H_6 + NH_3 \rightarrow [H_2B(NH_3)_2]^+ [BH_4]^-$
	$B_2H_6 + NH_3 \rightarrow H_2B = NH_2 + H_2$
	$B_2H_6 + NH_3 \rightarrow B_3N_3H_6 + H_2 + \text{solid boranes}$
	$B_2H_6 + NH_3 \rightarrow (BNH)_n + H_2$
	$B_2H_6 + NH_3 \rightarrow BN + H_2$

Table IV.

Wavenumber [cm ⁻¹]	Band assignment
780	NH ₂ def
1060	BH ₄ ⁻ ions antisymmetric bend
1160	BH ₄ ⁻ ions symmetric bend
1370	NH ₃ symmetric bend
1610	NH ₃ antisymmetric bend
2300	BH ₄ ⁻ ions antisymmetric stretch, broad absorption
3170	N-H symmetric stretch
3250	N-H antisymmetric stretch

Table V.

Wavenumber [cm ⁻¹]	Band assignment
608	BH ₂ rock
1338	B=N stretch
1620	NH ₂ symmetric bend
2499	B-H symmetric stretch
2568	B-H antisymmetric stretch
3437	N-H symmetric stretch
3519	N-H antisymmetric stretch

Table VI.

Wavenumber [cm ⁻¹]	Mode Assignments
780	B-N-B bending mode (out-of plane), sp ² bond
905	B-H bending mode (out-of -plane)
1100	transveral optical mode (TO), sp ³ bond
1380	B-N stretch mode (in-plane), sp ² bond
2520	B-H stretch mode
3430	N-H stretch mode

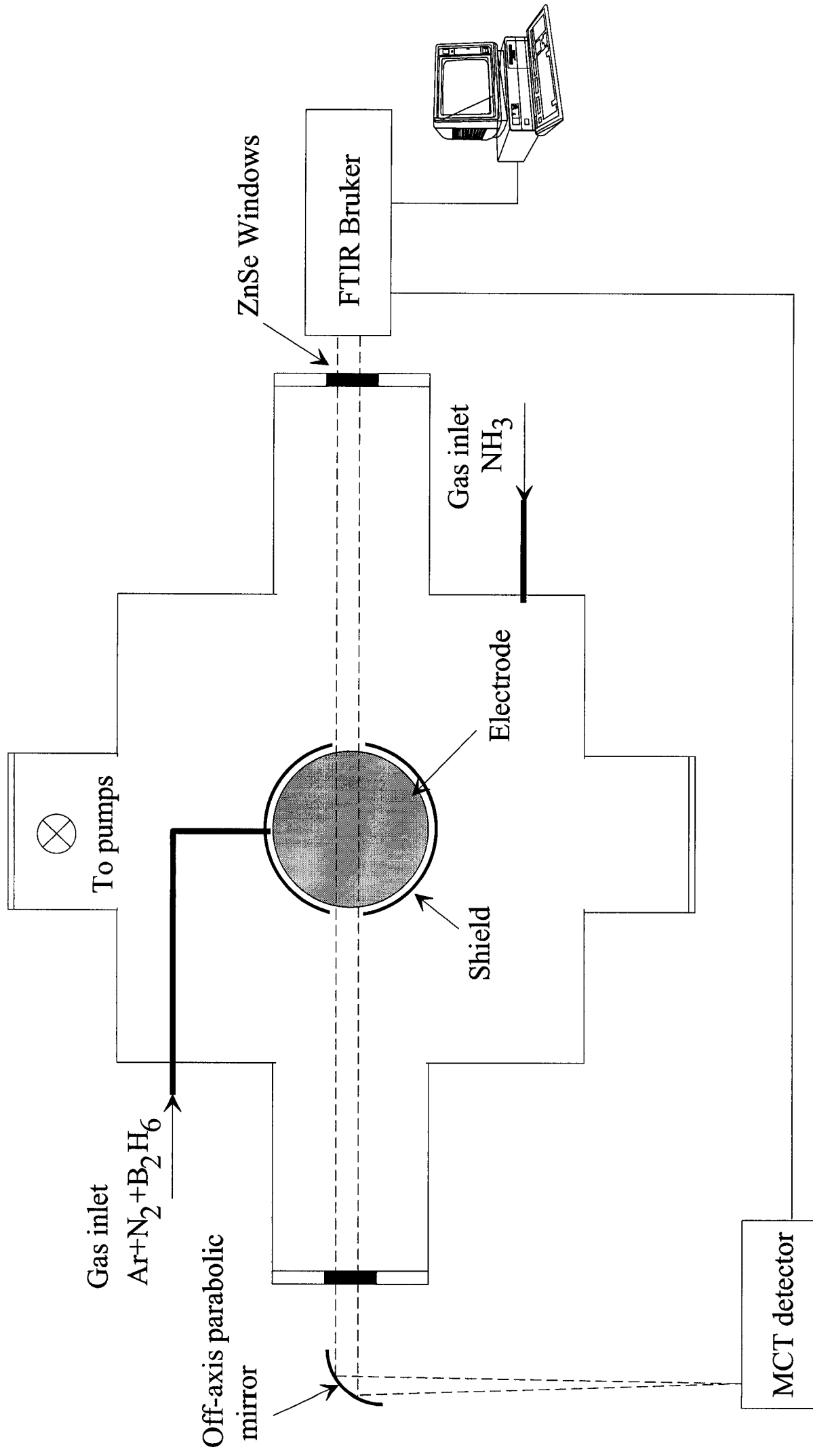


Fig. 1

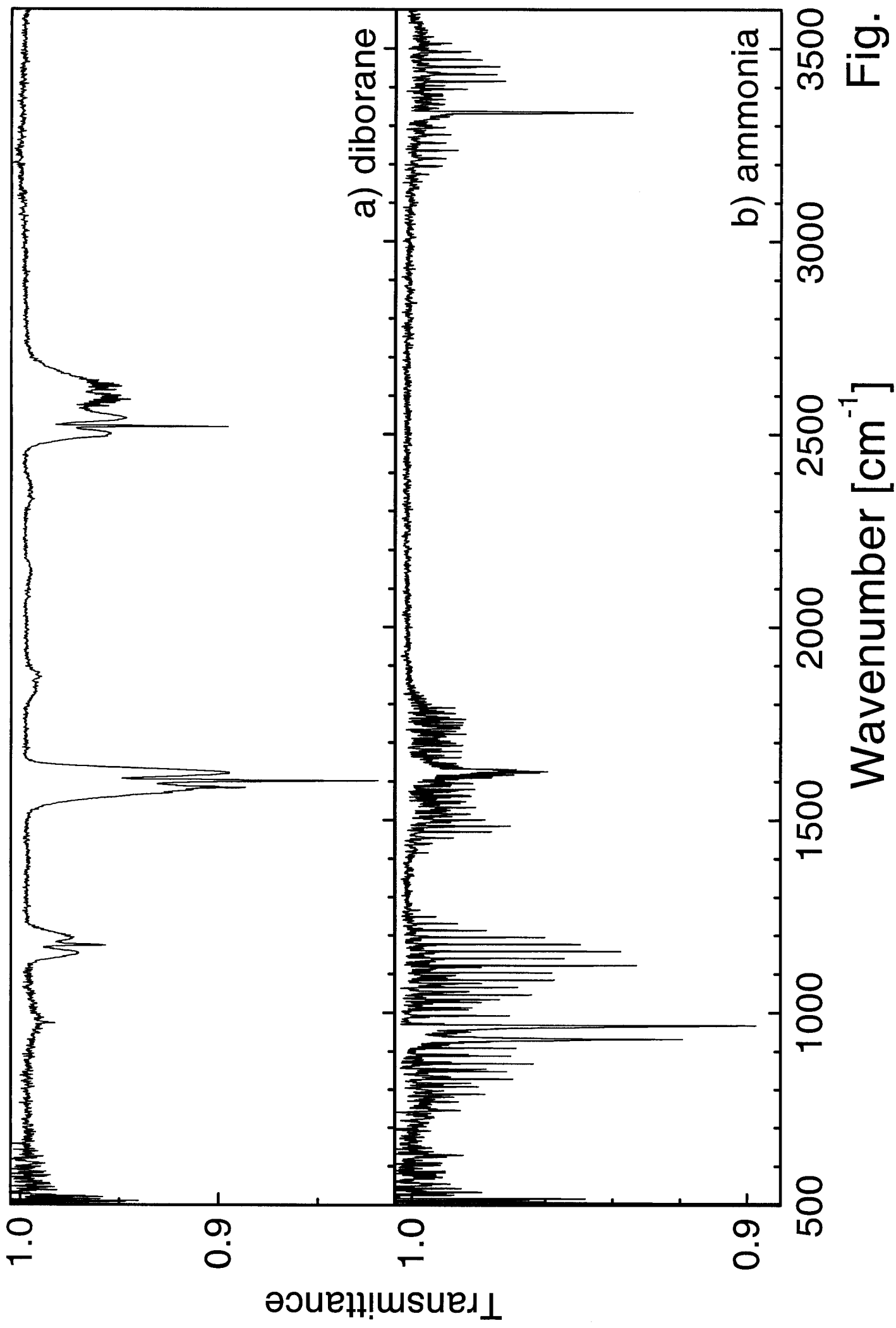


Fig. 2

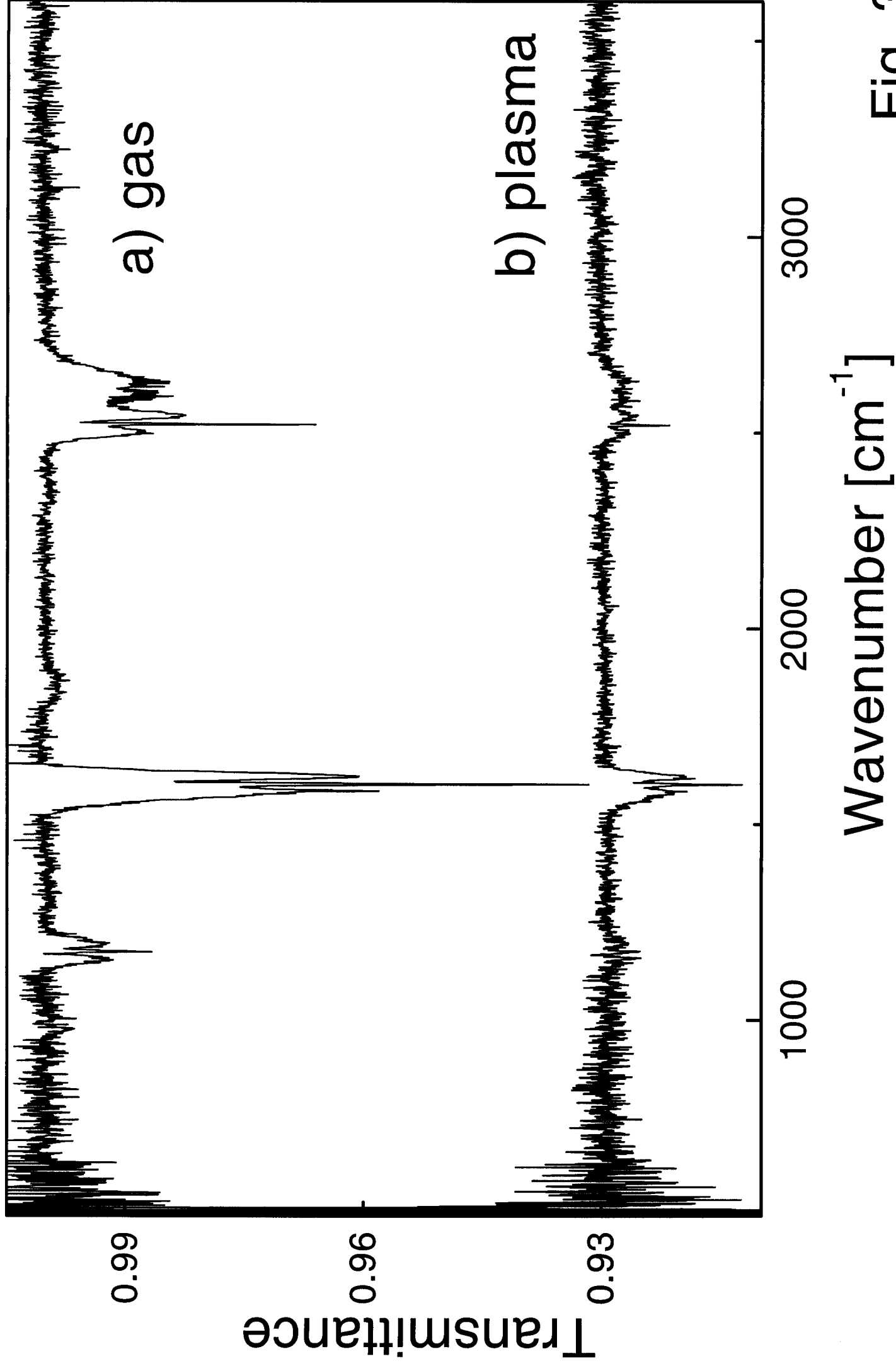


Fig. 3

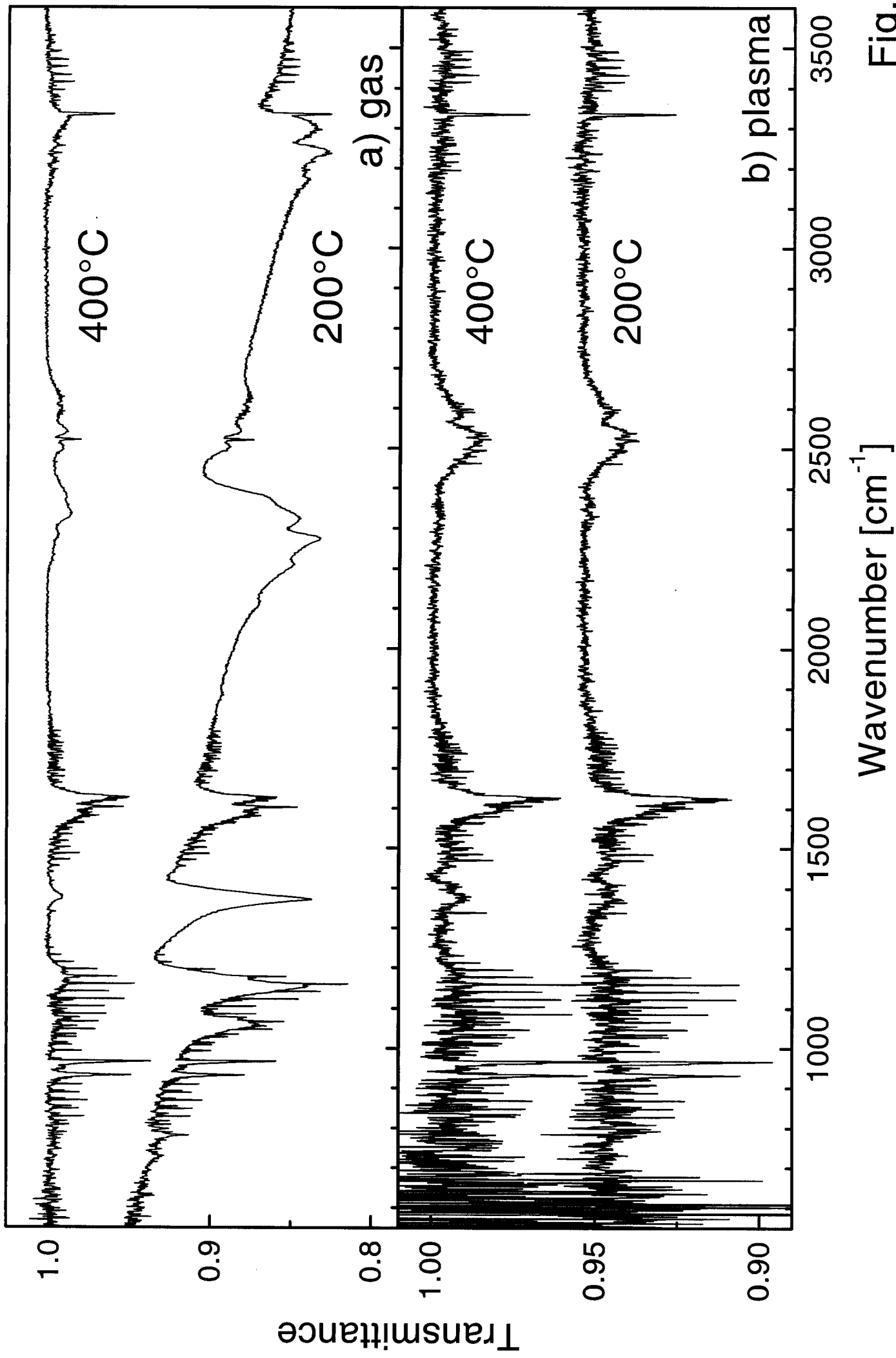


Fig. 4

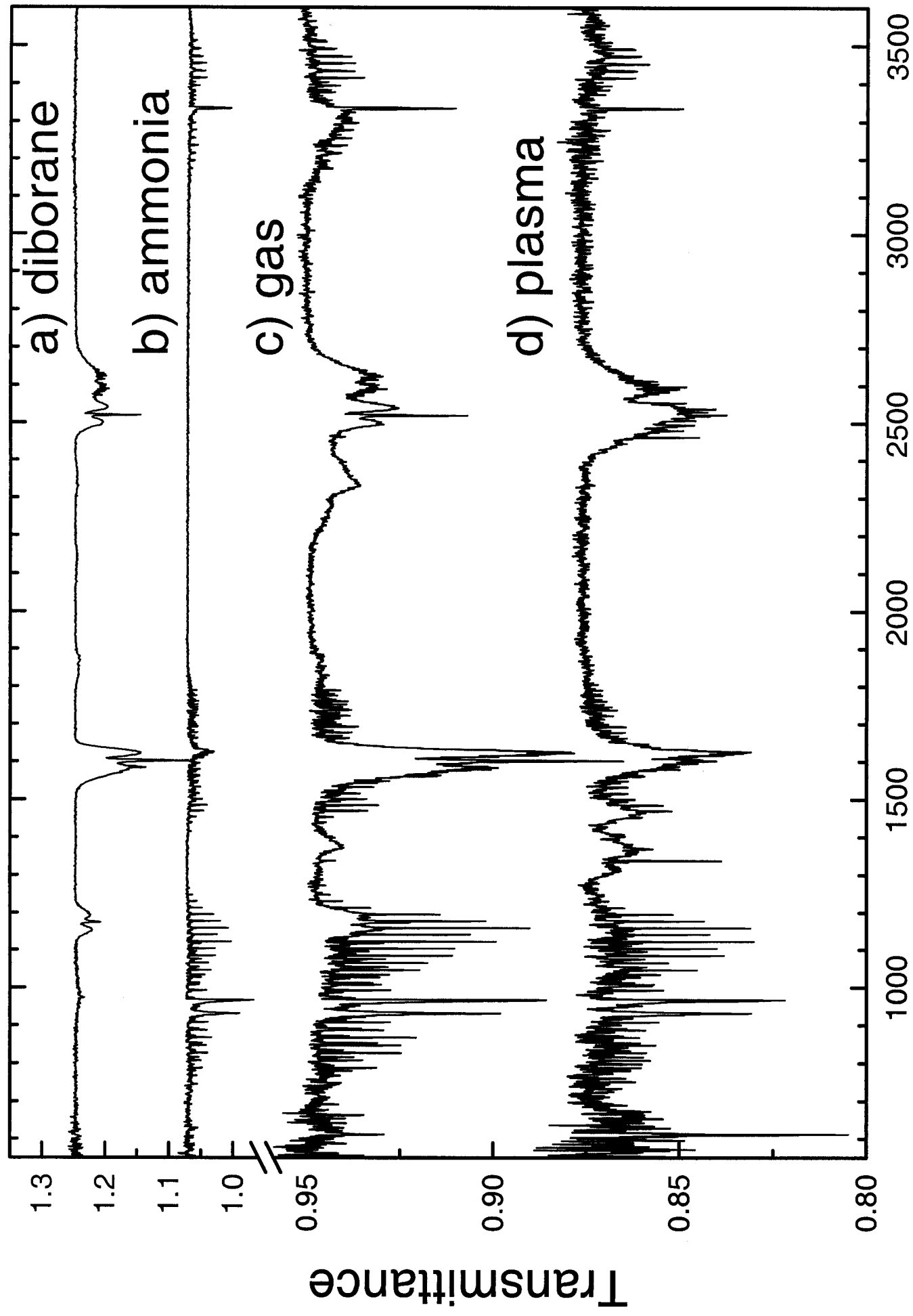
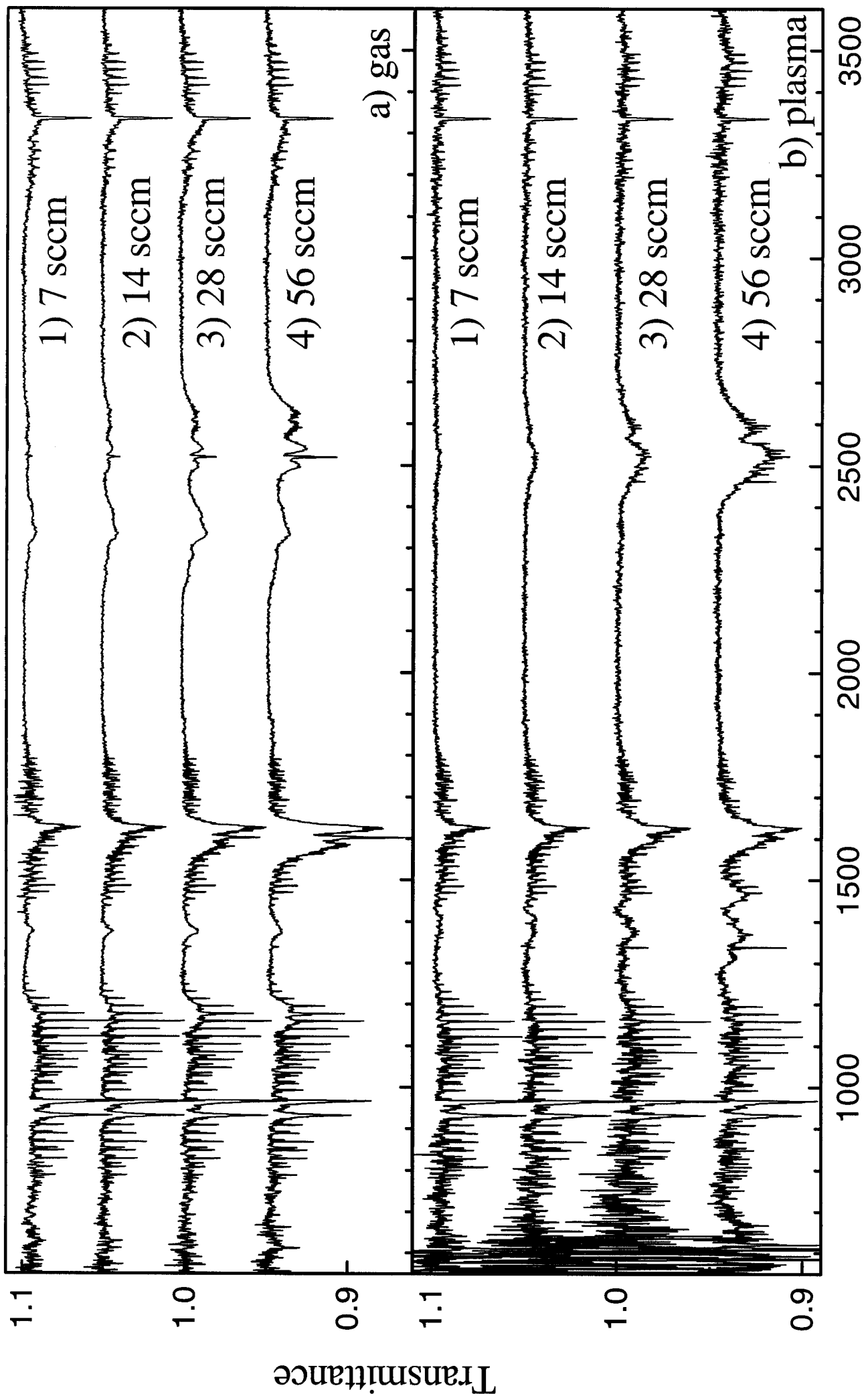


Fig. 5 Wavenumber [cm^{-1}]



Wavenumber [cm^{-1}]

Fig. 6

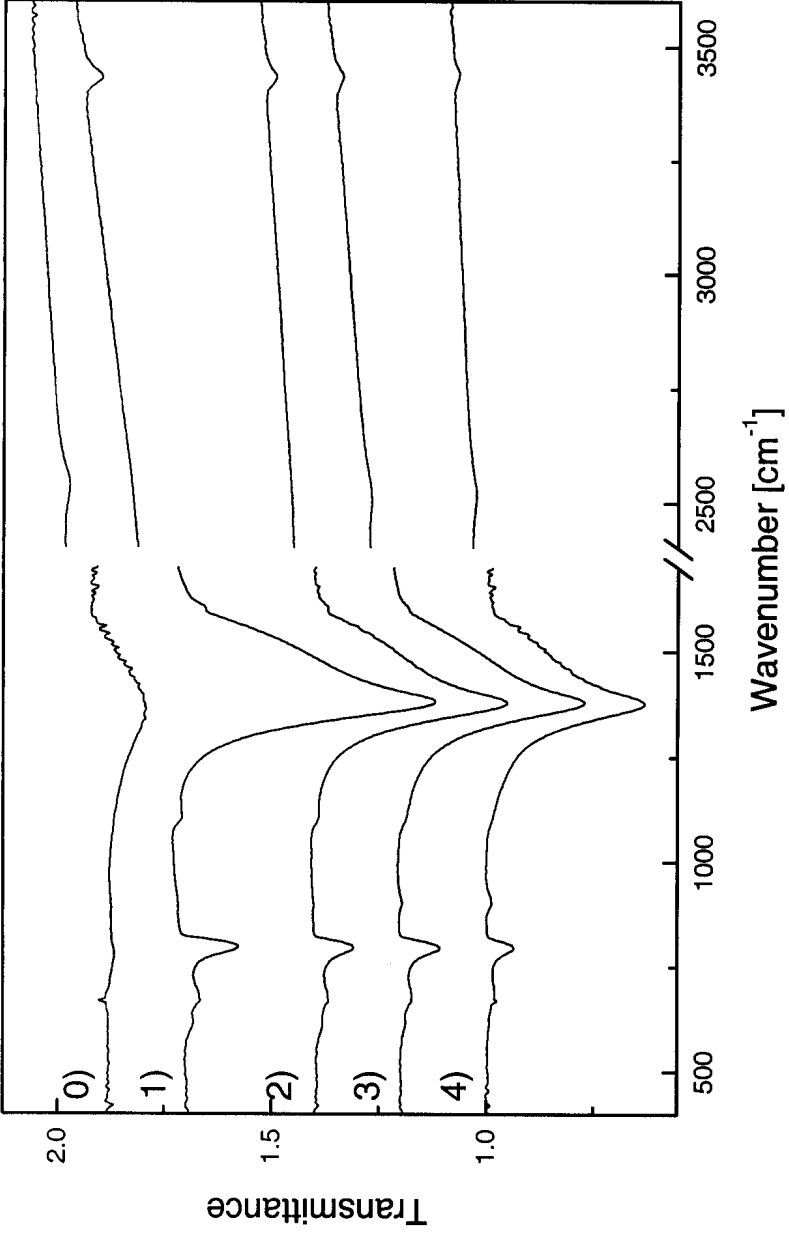


Fig. 7

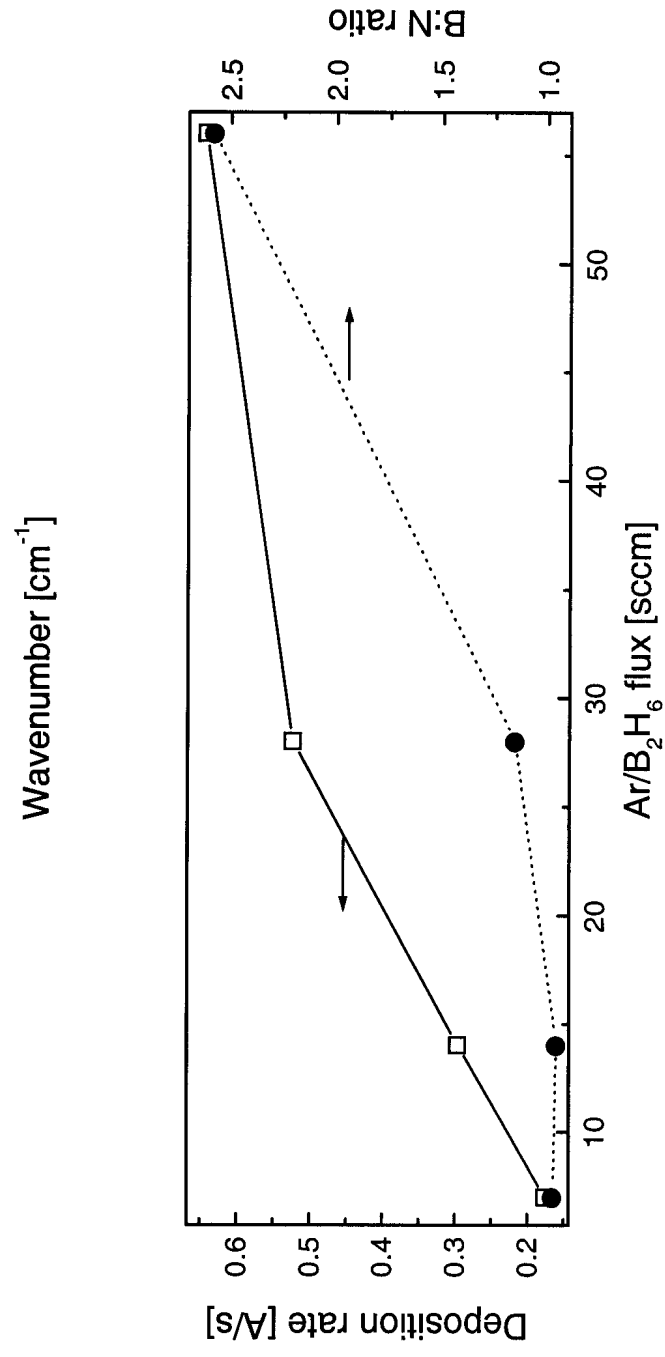


Fig. 8